

Universal phase diagrams for the quantum spin Hall systems

Shuichi Murakami^{1,2,*} and Shun-ichi Kuga³

¹*Department of Physics, Tokyo Institute of Technology,
2-12-1 Ookayama, Meguro-ku, Tokyo 152-8551, Japan*

²*PRESTO, Japan Science and Technology Agency (JST), Kawaguchi, Saitama, 332-0012, Japan*

³*Department of Applied Physics, University of Tokyo,
7-3-1 Hongo, Bunkyo-ku, Tokyo 113-8656, Japan*

We describe how the three-dimensional quantum spin Hall phase arises from the insulator phase by changing an external parameter. In 3D systems without inversion symmetry, a gapless phase should appear between the two phases with a bulk gap. The gapless points are monopoles and antimonopoles (in \mathbf{k} space), whose topological nature is the source of this gapless phase. In general, when the external parameter is changed from the ordinary insulator phase, two monopole-antimonopole pairs are created and the system becomes gapless. The gap-closing points (monopoles and antimonopoles) then move in the \mathbf{k} space as the parameter is changed further. They eventually annihilate in pairs, with changing partners from the pair creations, and the system opens a gap again, entering into the quantum spin Hall phase.

PACS numbers: 73.43.-f, 72.25.Dc, 73.43.Nq 85.75.-d

I. INTRODUCTION

Spin Hall effect (SHE)^{1,2} has been attracting current interest, because it enables us to produce spin current without magnetic field or magnet. The key aspect of this phenomenon is that the spin current is time-reversal invariant, unlike the spin itself. Due to this fact, the spin current can be induced without breaking the time-reversal symmetry. The physics of spin current opens up a new field for the spintronics.

In addition to the SHE in metals and doped semiconductors, SHE in insulators³, including the quantum spin Hall (QSH) effect^{4,5,6}, has been studied intensively. The quantum spin Hall phase in two dimensions (2D) is gapped in the bulk, while it has gapless edge modes carrying spin current without breaking time-reversal symmetry. The interesting point is that these edge modes are topologically protected. They are robust against weak disorder or interaction^{7,8}. Although edge states are usually sensitive to boundary conditions such as surface roughness and impurities, the present gapless edge states survive even if the boundary condition is changed. This topological protection comes from topological order in the bulk, which is characterized by the Z_2 topological number ν . ν takes only two values two values $\nu \equiv 0 \pmod{2}$ (ν =even) and $\nu \equiv 1 \pmod{2}$ (ν =odd). $\nu \equiv 0$ and $\nu \equiv 1$ correspond to the ordinary insulator (I) phase and the QSH phase, respectively. The Z_2 topological number ν represents the number of Kramers pairs of edge states. This phase has been proposed theoretically in bismuth thin film⁹. It has also been proposed theoretically in CdTe/HgTe/CdTe quantum well¹⁰, and it was demonstrated experimentally¹¹. Similar effect has been proposed theoretically for three dimensions (3D)^{12,13}, and is demonstrated in Bi_{0.9}Sb_{0.1}¹⁴. The following property of the Z_2 topological number is important. When the bulk states are gapped, this topological number will not change as far as the interaction or nonmagnetic disorder

is not strong enough to close the bulk gap, or to break to time-reversal symmetry spontaneously.

We note that the Z_2 topological number is encoded in the physics of gap-closing. The Z_2 topological number is defined as a Pfaffian of the matrix of the time-reversal operator, which involves the phase of the wavefunctions over the whole Brillouin zone. Its calculation is involved, and its physical meaning is hard to understand in an intuitive way. On the other hand, if we focus on the change of the Z_2 topological number occurring at the QSH-I phase transition, the change involves only the local information in the \mathbf{k} space, and is much simpler. Thus by studying how the phase transition between the QSH and the ordinary insulating phases occur, we can get deeper insight into the Z_2 topological number. This transition necessarily accompanies closing of the bulk gap. We note that the gap closing is not so trivial as it looks. Suppose we change one parameter in the system and check whether the gap closes or not. Because of the level repulsion, in many cases the gap does not close due to various matrix elements for interband hybridization. These matrix elements should vanish simultaneously, in order to close the gap. In some exceptional cases the gap closes; the conditions for the exceptional cases are related with the Z_2 topological number, and these are what we pursue in this paper.

In the theory of gap closing by tuning an external parameter, momenta which satisfy $\mathbf{k} \equiv -\mathbf{k} \pmod{\mathbf{G}}$ play an important role, where \mathbf{G} is a reciprocal lattice vector. Such momenta are called the time-reversal invariant momenta (TRIM) $\mathbf{\Gamma}_i$, and have the values $\mathbf{\Gamma}_{i=(n_1 n_2 n_3)} = (n_1 \mathbf{b}_1 + n_2 \mathbf{b}_2 + n_3 \mathbf{b}_3)/2$ in 3D, and $\mathbf{\Gamma}_{i=(n_1 n_2)} = (n_1 \mathbf{b}_1 + n_2 \mathbf{b}_2)/2$ in 2D, where $n_j = 0, 1$ and \mathbf{b}_j are primitive reciprocal lattice vectors. The TRIM are the momenta with $\mathbf{\Gamma}_i = \mathbf{G}/2$ where \mathbf{G} is a reciprocal lattice vector including zero vector. The TRIM are crucial in the sense that they are invariant under time reversal. It has been revealed through the research of

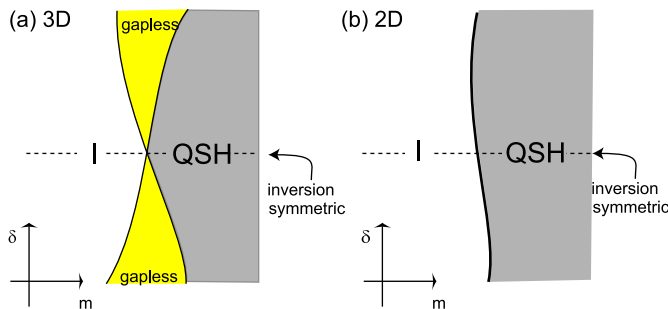


FIG. 1: (Color online) Phase diagram for the quantum spin Hall (QSH) and insulator (I) phases in (a) 3D and (b) 2D. m is a parameter driving the phase transition, and δ represents breaking of inversion symmetry. $\delta = 0$ corresponds to the inversion-symmetric system.

Z_2 topological numbers^{4,15} and gap-closing^{16,17} that the situation is quite different between the systems with and without inversion- (\mathcal{I} -) symmetry

By studying the gap-closing, one can see how the phase transition between the QSH and insulator phases occurs. We studied the 2D system in Ref. 16, and we have obtained the universal phase diagram (Fig. 1 (b)). The 3D system is studied in Ref. 17 and we give a handwaving argument to deduce the universal phase diagram in 3D, as shown in Fig. 1 (a). However, general theory for the 3D systems is still lacking, particularly for the \mathcal{I} -asymmetric systems. In this paper we describe the phase transition between the QSH and insulator phases in 3D and characterize its topological nature in a generic context. We describe the gap closing in the \mathbf{k} space for \mathcal{I} -asymmetric systems. From the topological characterization in this paper, we prove that the gapless phase necessarily comes in between the two phases. This paper is organized as follows. In Section II we describe how the phase transition between the quantum spin Hall and insulator phases occurs. Section III is devoted to a calculation on the three-dimensional Fu-Kane-Mele model to verify the results in the previous section. In Section IV we give conclusions and discussions.

We henceforth consider only clean systems without any impurities or disorder, while the effects of impurities and disorders will be discussed briefly in Section IV. The time-reversal symmetry is assumed throughout the paper. Our analysis here assumes that the Hamiltonian is generic, and we exclude the Hamiltonians which require fine tuning of parameters. In other words, we exclude the cases which are vanishingly improbable as a real material.

II. PHASE TRANSITION BETWEEN THE QUANTUM SPIN HALL AND INSULATOR PHASES

As we found in Ref. 16, in 2D \mathcal{I} -symmetric systems, the gap closing at the QSH-I transition occurs at TRIM $\mathbf{k} = \Gamma_i$. This corresponds to the expression of the Z_2

topological number as a product of the parity eigenvalues over all the TRIMs $\mathbf{k} = \Gamma_i$ over the occupied states¹⁵; namely at the transition the conduction and valence bands with opposite parities exchange their parities and the Z_2 topological number changes. On the other hand, for \mathcal{I} -asymmetric 2D systems, the gap closes at $\pm\mathbf{k}_0 + \Gamma_i$ ($\mathbf{k}_0 \neq 0$) by tuning some parameter. In correspondence with this gap closing, the Z_2 topological number should be expressed as an integral over the \mathbf{k} space. This is indeed the Pfaffian expression of the Z_2 topological number^{4,15}.

The phase transition in 3D^{12,13} can be studied similarly to 2D¹⁶. The generic phase diagram in 3D is shown in Fig. 1(a) and is different from 2D (Fig. 1(b)). In \mathcal{I} -asymmetric 3D systems, gapless phase emerges¹⁷, which is nonexistent in 2D. This gapless phase arises from a topological nature of the gap-closing points in 3D. Namely the gap-closing points in 3D \mathbf{k} space are monopoles and antimonopoles, whose “monopole charges” are conserved. This conservation restricts the form of the QSH-I phase transition, as we see in this paper.

A. General description of the QSH-I phase transition in 3D

Because the QSH results from the spin-orbit coupling, the Z_2 topological number ν is $\nu = 0 \bmod 2$, when the spin-orbit coupling is zero. When we think of switching on the spin-orbit coupling, some may undergo a phase transition to the QSH phase. This phase transition changes the Z_2 topological number, which means that it is accompanied by a closing of the bulk gap. Thus to search for candidate materials for the QSH phase, we consider tuning of a single parameter to drive the phase transition. Let us call the parameter m .

As we mentioned previously^{16,17}, the phase transition is different whether the system considered is (i) \mathcal{I} -symmetric or (ii) \mathcal{I} -asymmetric. The reason for the difference is the following. When (i) the \mathcal{I} -symmetry is present, all the states are doubly degenerate due to Kramers theorem. The problem is how many parameters should be tuned to close the gap between the conduction band and the valence band, which are both doubly degenerate. This number is called a codimension, and in this case it is five, which exceeds the number of parameters (\mathbf{k}, m) . Namely there are five independent parameters for hybridization between the valence and conduction bands, and unless they are finely tuned to be zero simultaneously, the gap never close, and the phase transition does not occur. This is interpreted as level repulsion between the valence and conduction bands.

Nevertheless, there is an exceptional case in (i) \mathcal{I} -symmetric systems. At TRIM $\mathbf{k} = \Gamma_i$, all the states are classified in terms of the parity eigenvalues ($= \pm 1$). When the valence and conduction bands have the same

parities, the Hamiltonian becomes¹⁷

$$H(\mathbf{k}) = E_0(\mathbf{k}) + \sum_{i=1}^5 a_i(\mathbf{k}) \Gamma_i, \quad (1)$$

where a_i 's and E_0 are real even functions of \mathbf{k} . Γ_i are 4×4 matrices given by $\Gamma_1 = 1 \otimes \tau_x$, $\Gamma_2 = \sigma_z \otimes \tau_y$, $\Gamma_3 = 1 \otimes \tau_z$, $\Gamma_4 = \sigma_y \otimes \tau_y$, and $\Gamma_5 = \sigma_x \otimes \tau_y$, where σ_i and τ_i are Pauli matrices. The gap closes when $a_i(\mathbf{k}) = 0$ for $i = 1, \dots, 5$. It means that the codimension is five, and the gap never closes in this case. On the other hand, when the valence and conduction bands have the opposite parities, the Hamiltonian reads¹⁷,

$$H(\mathbf{k}) = a_0(\mathbf{k}) + a_5(\mathbf{k}) \Gamma'_5 + \sum_{j=1}^4 b^{(j)}(\mathbf{k}) \Gamma'_j, \quad (2)$$

where $a_0(\mathbf{k})$ and $a_5(\mathbf{k})$ are even functions of \mathbf{k} , and $b^{(j)}(\mathbf{k})$ ($j = 1, 2, 3, 4$) are odd functions of \mathbf{k} . Here Γ'_i are 4×4 matrices given by $\Gamma'_1 = \sigma_z \otimes \tau_x$, $\Gamma'_2 = 1 \otimes \tau_y$, $\Gamma'_3 = \sigma_x \otimes \tau_x$, $\Gamma'_4 = \sigma_y \otimes \tau_x$, and $\Gamma'_5 = 1 \otimes \tau_z$. In this case the gap closes only when five equations $a_5(\mathbf{k}) = 0$, $b^{(j)}(\mathbf{k}) = 0$ are satisfied. At the TRIM, $b^{(j)}(\mathbf{\Gamma}_i)$ ($j = 1, 2, 3, 4$) identically vanish, and only one condition $a_5(\mathbf{\Gamma}_i) = 0$ remains to be satisfied. This means that the codimension is reduced to one. Thus if the valence and conduction bands have opposite parities, four matrix elements (out of five) for hybridization between the valence and conduction bands vanish identically. The resulting codimension, i.e. the number of parameters to be tuned for gap closing, is one. This is equal to the number of the tunable parameter, m . (We note that in this case \mathbf{k} is fixed to be $\mathbf{\Gamma}_i$.) To summarize the gap can close only at $\mathbf{k} = \mathbf{\Gamma}_i$ for \mathcal{I} -symmetric systems. This gap-closing occurs with an exchange of parities between the conduction and valence bands, as is similar to 2D.

On the other hand, (ii) if \mathcal{I} -symmetry is absent, the bands are not degenerate (except for the points with $\mathbf{k} = \mathbf{\Gamma}_i$). In this case the resulting codimension D_c is three^{17,18,19}, which is smaller than that in the inversion-symmetric case. This is because the bands are nondegenerate and the level repulsion is less stringent. In the symmetry classification of Wigner and Dyson^{20,21}, the \mathcal{I} -symmetry breaking makes the symmetry class from symplectic ($D_c = 5$) to unitary ($D_c = 3$). The codimension ($D_c = 3$) is less than the number of parameters (m, k_x, k_y, k_z). Thus the gap can close by tuning a parameter m .

B. Monopole-antimonopole pair creation and annihilation in \mathbf{k} space

Henceforth we focus on (ii) the \mathcal{I} -asymmetric systems. Our theory is based on the physics of gauge field in \mathbf{k} -space^{22,23}. When α -th band is degenerate with another band at an isolated point \mathbf{k} , such point is associated with

a monopole for the gauge field in \mathbf{k} -space. The gauge field $\mathbf{A}_\alpha(\mathbf{k})$ and the corresponding field strength $\mathbf{B}_\alpha(\mathbf{k})$ are defined as

$$\mathbf{A}_\alpha(\mathbf{k}) = -i \langle \psi_\alpha(\mathbf{k}) | \nabla_{\mathbf{k}} | \psi_\alpha(\mathbf{k}) \rangle, \quad (3)$$

$$\mathbf{B}_\alpha(\mathbf{k}) = \nabla_{\mathbf{k}} \times \mathbf{A}_\alpha(\mathbf{k}), \quad (4)$$

The monopole density is defined as

$$\rho_\alpha(\mathbf{k}) = \frac{1}{2\pi} \nabla_{\mathbf{k}} \cdot \mathbf{B}_\alpha(\mathbf{k}) \quad (5)$$

Though at first sight $\rho_\alpha(\mathbf{k})$ vanishes identically, because $\nabla_{\mathbf{k}} \cdot (\nabla_{\mathbf{k}} \times) = 0$, it is not true. In some cases where the α -th band touches with another band at some \mathbf{k} -point, the wavenumber cannot be chosen as a single continuous function for the whole Brillouin zone. In such case the Brillouin zone should be patched with more than one continuous wavefunctions²⁴, as is similar to the vector potential of the Dirac monopole²⁵. This allows a δ -function singularity of $\rho(\mathbf{k})$ at the band touching. As a result the monopole density has the form $\rho(\mathbf{k}) = \sum_l q_l \delta(\mathbf{k} - \mathbf{k}_l)$ where q_l is an integer called a monopole charge. Even when we vary the system by changing a parameter continuously, the monopole charge is conserved, because it is quantized. The only chance for the monopole charge to change is to create or to annihilate a pair of a monopole ($q_l = 1$) and an antimonopole ($q_{l'} = -1$). More detailed formulation is in Appendix A.

In the present case, we restrict ourselves to time-reversal symmetric cases, where we have

$$\mathbf{B}_\alpha(\mathbf{k}) = -\mathbf{B}_{\bar{\alpha}}(-\mathbf{k}), \quad \rho_\alpha(\mathbf{k}) = \rho_{\bar{\alpha}}(-\mathbf{k}), \quad (6)$$

where $\bar{\alpha}$ is the label which is a time-reversed label from α . It means that the monopoles distribute symmetrically with respect to the origin.

At the phase transition, the gap closes between a single valence band and a single conduction band at $\mathbf{k} = \mathbf{k}_0$. Instead of considering a general Hamiltonian it is sufficient and much simpler to consider a 2×2 matrix $H(\mathbf{k}, m)$. Here we introduce an external parameter m , which controls the phase transition. We note that the following discussion on 2×2 Hamiltonian is easily generalized to an arbitrary Hamiltonian. The 2×2 Hamiltonian $H(\mathbf{k}, m)$ is expanded as

$$H(\mathbf{k}, m) = a_0(\mathbf{k}, m) + \sum_{i=1}^3 a_i(\mathbf{k}, m) \sigma_i, \quad (7)$$

where σ_i ($i = 1, 2, 3$) are the Pauli matrices. The gap closes when the two eigenvalues are identical, i.e. when the three conditions $a_i(\mathbf{k}, m) = 0$ ($i = 1, 2, 3$) are satisfied. Therefore, in general, the gap-closing point in the (k_x, k_y, k_z, m) -hyperspace forms a curve, which we call a "string". Generally, this string C occupies a finite region in m -direction; namely, it is vanishingly improbable to lie in a single value of m . When we cut the string C at some value of m , the intersections in the \mathbf{k} -space are the points where the gap closes, namely, the

monopoles and antimonopoles. Thus the string C is the trajectory of the monopoles and antimonopoles. Because the monopole charge is conserved, the monopoles and antimonopoles are created and annihilated only in pairs, which means that the trajectory C of the monopoles and antimonopoles forms a closed loop in the (\mathbf{k}, m) space (see Fig. 8 in Appendix A). Namely, the string C has no end point, because an end point of C would violate the conservation of monopole charge.

Henceforth we describe how the phase transition occurs, thereby opening a gap. We consider a situation where one side of m , e.g. $m < m_0$ is gapped while the other side of m , e.g. $m > m_0$ is gapless. This means that the string C exists only in the $m > m_0$ region. In other words, we consider an extremum of the string C . We pick up a gap-closing point $(\mathbf{k}, m) = (\mathbf{k}_0, m_0)$, (i.e. $\mathbf{a}(\mathbf{k}_0, m_0) = 0$) and consider the vicinity of this point. We investigate conditions for the point (\mathbf{k}_0, m_0) to become an extremum of the string C . We expand the coefficients to the linear order

$$a_i(\mathbf{k}, m) = \sum_j M_{ij} \Delta k_j + N_i \Delta m, \quad (8)$$

or in a matrix form

$$\mathbf{a}(\mathbf{k}, m) = M \Delta \mathbf{k} + \Delta m \mathbf{N}, \quad (9)$$

where $\Delta k_j = k_j - k_{0j}$, $\Delta m = m - m_0$, $M_{ij} = \left. \frac{\partial a_i}{\partial k_j} \right|_0$ and $N_i = \left. \frac{\partial a_i}{\partial m} \right|_0$. If the determinant of the matrix M does not vanish, the gap-closing condition, $\mathbf{a} = (a_1, a_2, a_3) = 0$ gives

$$\Delta \mathbf{k} = -M^{-1} \mathbf{N} \Delta m. \quad (10)$$

It means that a gap-closing point moves as the parameter m changes, and it exists on the both sides of $m = m_0$. It is not the case of our interest. Therefore we conclude

$$\det M \equiv \det_{(i,j)} \left. \frac{\partial a_i}{\partial k_j} \right|_0 = 0, \quad (11)$$

which is imposed in addition to $a_i = 0$. Thus there are four conditions in total, which give a set of gap-closing points (\mathbf{k}_0, m_0) located at an extremum of the string C .

We now calculate behaviors of the system in the vicinity of (\mathbf{k}_0, m_0) . If Eq. (11) holds, the matrix M has a normalized eigenvector \mathbf{n}_1 with null eigenvalue: $M \mathbf{n}_1 = 0$. From \mathbf{n}_1 we consider two additional unit vectors \mathbf{n}_α ($\alpha = 2, 3$) to form an orthonormal basis $\{\mathbf{n}_1, \mathbf{n}_2, \mathbf{n}_3\}$. We adopt this basis for the \mathbf{k} space;

$$\Delta \mathbf{k} = U \Delta \mathbf{p} \equiv (\mathbf{n}_1, \mathbf{n}_2, \mathbf{n}_3) \begin{pmatrix} \Delta p_1 \\ \Delta p_2 \\ \Delta p_3 \end{pmatrix}. \quad (12)$$

Namely, $(\Delta p_1, \Delta p_2, \Delta p_3)$ is a coordinate rotated from $(\Delta k_1, \Delta k_2, \Delta k_3)$. From (9) and (12) to the linear order in $\Delta \mathbf{k}$ and m , we have

$$\mathbf{a} = \Delta p_2 \mathbf{u}_2 + \Delta p_3 \mathbf{u}_3 + \Delta m \mathbf{N}, \quad (13)$$

where $\mathbf{u}_i = M \mathbf{n}_i$ ($i = 2, 3$). Up to this order, the gap closing condition, $\mathbf{a} = 0$, has no nontrivial solution in general, because the three vectors $\mathbf{u}_2, \mathbf{u}_3, \mathbf{N}$ are generally linearly independent. It is not the case of our interest. Thus we have to include the next order in $\Delta \mathbf{k}$ and Δm , to see whether the gap closes for $\Delta m \neq 0$;

$$\begin{aligned} \mathbf{a} = & \Delta m \mathbf{N} + \Delta p_2 \mathbf{u}_2 + \Delta p_3 \mathbf{u}_3 + \sum_{i,j=1,2,3, i \leq j} \mathbf{u}_{ij} \Delta p_i \Delta p_j \\ & + \sum_{i=1}^3 \tilde{\mathbf{u}}_i \Delta m \Delta p_i + \mathbf{u} (\Delta m)^2, \end{aligned} \quad (14)$$

where $\mathbf{u}_{ij}, \tilde{\mathbf{u}}_i$ and \mathbf{u} are vectors. We first look at the gap-closing point $\mathbf{a} = 0$. We put $\Delta m \propto \lambda$ where λ is small, and investigate the order of λ for each term. As we have seen, if Δp_i ($i = 1, 2, 3$) are of the order λ , the gap-closing condition has no nontrivial solution. The reason is that the right-hand side of Eq. (14) has no term linear in Δp_1 . Hence we have to consider the quadratic term in Δp_1 , for which we put $\Delta p_1 \propto \lambda^{1/2}$. Then up to $O(\lambda)$ we have

$$\Delta m \mathbf{N} + \Delta p_2 \mathbf{u}_2 + \Delta p_3 \mathbf{u}_3 + (\Delta p_1)^2 \mathbf{u}_{11} = 0. \quad (15)$$

The solution is given by

$$\begin{pmatrix} (\Delta p_1)^2 \\ \Delta p_2 \\ \Delta p_3 \end{pmatrix} = -\Delta m (Q^{-1} \mathbf{N}), \quad Q = (\mathbf{u}_{11}, \mathbf{u}_2, \mathbf{u}_3). \quad (16)$$

Because $\Delta p_1^2 \geq 0$, the solution for this exists only when Δm has the same sign with $-(Q^{-1} \mathbf{N})_1$. This means that on one side of $\Delta m = 0$ the system is gapped, while on the other side the system has gapless points,

$$\Delta p_1 = \pm \sqrt{-(Q^{-1} \mathbf{N})_1 \Delta m}, \quad (17)$$

$$\Delta p_2 = -(Q^{-1} \mathbf{N})_2 \Delta m, \quad (18)$$

$$\Delta p_3 = -(Q^{-1} \mathbf{N})_3 \Delta m. \quad (19)$$

Thus when Δm is changed across zero, monopole-antimonopole pairs are created and dissociate along the Δp_1 direction. The trajectory of the gapless points is as shown in Fig. 2. This is exactly the case of our pursuit: the point of an extremum of the gap-closing. Thus we have shown that for given Hamiltonian with broken \mathcal{I} -symmetry, such point exists in general, and the behavior of the gapless points in the vicinity of this pair creation or annihilation is described.

Next we consider the dispersion around the gap-closing point. Around the monopole the dispersion is linear in \mathbf{k} . It is, however, not the case around the point of monopole-antimonopole pair creation. From Eq. (14), we can derive \mathbf{k} dependence of the gap at $\Delta m = 0$ (pair creation or annihilation). The gap is given by $E_g = 2|\mathbf{a}|$. Hence, for $\Delta m = 0$. The gap behaves as

$$E_g \propto \Delta p_2, \Delta p_3, (\Delta p_1)^2 \quad (20)$$

Thus the dispersion along the Δp_1 direction is quadratic, while that along the Δp_2 and Δp_3 directions is linear. The Δp_1 -direction is the direction for the monopole-antimonopole pair to dissociate.

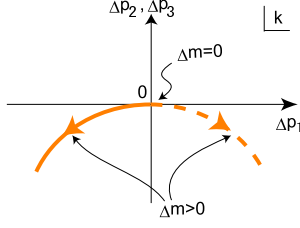


FIG. 2: (Color online) Trajectory for the gapless points in the \mathbf{k} space. At $m = m_0$ a monopole-antimonopole pair is created, and they run to the opposite directions when m is changed. We assume $(Q^{-1}\mathbf{N})_1 < 0$, in which gapless points exist only for $\Delta m \geq 0$.

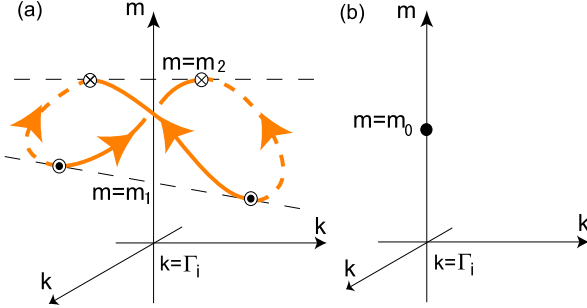


FIG. 3: (Color online) Trajectory of the gapless points for (a) inversion-asymmetric and (b) symmetric systems. For (b) inversion-symmetric systems, the gapless point is located at $\mathbf{k} = \Gamma_i$, and is an isolated point in the m - \mathbf{k} space. Only at $m = m_0$ the system is gapless. For (a) inversion-asymmetric systems, on the other hand, the gapless points are created in monopole-antimonopole pairs at $m = m_1$, and move in \mathbf{k} -space as m is varied. The system opens a gap only by pair annihilation of these gapless points at $m = m_2$.

C. Change in the Z_2 topological numbers

According to Ref. 12, the Z_2 topological numbers ν_j ($j = 0, 1, 2, 3$) in 3D are defined as

$$(-1)^{\nu_0} = \prod_{n_j=0,1} \delta_{n_1 n_2 n_3}, \quad (21)$$

$$(-1)^{\nu_{i=1,2,3}} = \prod_{n_j \neq i=0,1; n_i=1} \delta_{n_1 n_2 n_3}, \quad (22)$$

where

$$\delta_i = \sqrt{\det[w(\Gamma_i)]} / \text{Pf}[w(\Gamma_i)] = \pm 1. \quad (23)$$

Here $w_{nm} = \langle u_{m,-\mathbf{k}} | \Theta | u_{n,\mathbf{k}} \rangle$, where Θ is the time-reversal operator, and $u_{m,\mathbf{k}}$ is the periodic part of the Bloch wavefunction. Each phase is expressed as $\nu_0; (\nu_1 \nu_2 \nu_3)$, which distinguishes 16 phases. Because among ν_i , ν_0 is the only topological number which is robust against disorder, the phases are mainly classified by ν_0 . When ν_0 is odd the phase is called as the strong topological insulator (STI), while if it is even it is called the weak topological insulator (WTI). The STI and WTI

correspond to the QSH and I phases, respectively. The other indices ν_1 , ν_2 , and ν_3 are used to distinguish various phases in the STI or WTI phases, and each phase can be associated with a mod 2 reciprocal lattice vector $\mathbf{G}_{\nu_1 \nu_2 \nu_3} = \nu_1 \mathbf{b}_1 + \nu_2 \mathbf{b}_2 + \nu_3 \mathbf{b}_3$, as was proposed in Ref. 12.

We can relate the shape of the trajectory (“loop”) of the gapless points with the change in the topological number. To see this, we note the following. From Eqs. (21) and (22), the Z_2 topological numbers in 3D are defined on planes $S_i^{(n_i)}: \mathbf{k} \cdot \mathbf{a}_i = \pi n_i$ with $n_i = 0, 1$ in the Brillouin zone as

$$\nu_0 \equiv \prod_{\Gamma_j} \delta_j, \quad \nu_i \equiv \prod_{\Gamma_j \in S_i^{(1)}} \delta_j, \quad (24)$$

which are gauge invariant and have the values ± 1 .

Let us take the plane $S_1^{(1)}$ for example. This affects the numbers ν_0 and ν_1 . Based on the theory on homotopy characterization of the 2D QSH phase¹³, one can show the following. An intersection of the loops with the plane $S_1^{(1)}$ forms a set of isolated points. They are symmetric with respect to $\mathbf{k} = \Gamma_{(100)}$, and the number of points is even. When the number of the points is $2(2N + 1)$ (N : integer), then it accompanies the change in the Z_2 topological number ν_0 and ν_1 . Otherwise, when the number is $4N$ (N : integer), then it does not accompany the change in the Z_2 topological numbers. To show this we note the result in Ref. 13: in 2D the Z_2 topological number ν is equal (modulo 2) to an integral of the Berry curvature inside a half of the Brillouin zone plus an extra term coming from “contraction” of the Brillouin zone¹³. We can regard the slice of the 3D Brillouin zone by $S_1^{(1)}$ as a 2D Brillouin zone¹³, which we call $D_1^{(1)}$. By this identification we treat the 3D Z_2 topological numbers in the same way as in 2D. When the loop intersects the half of the Brillouin zone $D_1^{(1)}$ (within $S_1^{(1)}$) once, it means that at some m the monopole passes through the half of the Brillouin zone $D_1^{(1)}$, and changes the integral of the Berry curvature by unity. Thus it changes ν_0 and ν_1 as $\nu_0 \rightarrow \nu'_0 \equiv \nu_0 + 1 \pmod{2}$, $\nu_1 \rightarrow \nu'_1 \equiv \nu_1 + 1 \pmod{2}$. Therefore if $2N + 1$ intersections occur within the half of $D_1^{(1)}$, the Z_2 topological numbers ν_0 and ν_1 changes (odd \leftrightarrow even), while if $2N$ intersections occur, ν_0 and ν_1 are unchanged. This completes the proof that when a number of intersections between the loops and the plane $S_1^{(1)}$ is $2(2N + 1)$ (N : integer), it accompanies the change in the Z_2 topological numbers, whereas $4N$ intersections involve no change in the Z_2 topological numbers.

For further investigation, we consider the following example. Suppose we consider simultaneous pair creations at $m = m_1$, and $\mathbf{k} = \pm \mathbf{k}_0 + \Gamma_i$. As a result we have two monopoles and two antimonopoles. Eventually these will be annihilated at $\mathbf{k} = \pm \mathbf{k}'_0 + \Gamma_i$. Then there are two possible cases: pair annihilation occurs (A) with changing partners (Fig. 3(a)) and (B) without changing the partners (Fig. 4). We can show that (A) changes the Z_2 topological numbers while (B) does not. One can see the

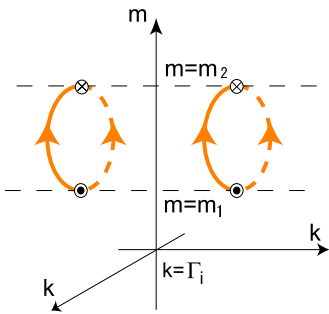


FIG. 4: (Color online) Trajectory of the gapless points for inversion-asymmetric systems, but without the phase transition.

reason in two different ways. One way to see the difference is to consider an intersection of the “loops” with the planes such as $S_i^{(ni)}$. In this case, on half of the Brillouin zone the number of intersection points is necessarily even.

The other way to see this difference between (A) and (B) is to consider switching on a perturbation which restores the \mathcal{I} -symmetry. One may wonder whether it is possible to restore the \mathcal{I} -symmetry without encountering a phase transition. When \mathcal{I} -symmetry-breaking term in the Hamiltonian is sufficiently small, it is possible, whereas in generic systems we cannot prove that it is possible. Therefore, in the following we assume that it is possible to restore the \mathcal{I} -symmetry without encountering a phase transition. In this case, the gapless loop eventually reduces to a point in (A) (Fig. 3(a)). Meanwhile in the case (B) (Fig. 4) the loops cannot reduce to a point in the \mathcal{I} -symmetric limit. In the case (B), by restoring the \mathcal{I} -symmetry, each of the two loops seems to shrink to a point ($\neq \Gamma_i$); this, however, is impossible because in \mathcal{I} -symmetric case the gap closing does not occur at $\mathbf{k} \neq \Gamma_i$ due to the large codimension ($= 5$). Thus in (B), the perturbation can get rid of the gapless points completely from the (\mathbf{k}, m) space, i.e. the two phases of both sides are identical.

From these arguments one can see that the change of ν_0 is equal to the number of loops in m - \mathbf{k} space, modulo 2. In the case (A) (Fig. 3(a)), there is a single loop, and the change of ν_0 is one, while in the case (B) (Fig. 4), the number of loop is two, and ν_0 is unchanged.

In the analysis in this section, we assumed that as the external parameters are changed, the Hamiltonian and the band structure change continuously. Namely, we assumed an absence of first-order transitions. Whether or not first-order transitions happen depends on details of the system and is not solely determined by system symmetries and topological order. Therefore, if first-order transitions are taken into account, it is no longer possible to discuss universal properties. For example, when first-order transitions are allowed, the two phases, QSH and I phases, can transit to each other via first-order transition without closing a bulk gap. This situation is realized in the model in Ref. 26, where the topological QSH phase is

realized as a phase with spontaneously broken symmetry.

III. EXAMPLE: 3D FU-KANE-MELE MODEL

To confirm the topological discussion in the previous section, we take the 3D model proposed by Fu, Kane and Mele¹² on a diamond lattice as an example. This model shows a transition between STI and WTI. The model is written as

$$H = t \sum_{\langle ij \rangle} c_i^\dagger c_j + i(8\lambda_{\text{SO}}/a^2) \sum_{\langle\langle ij \rangle\rangle} c_i^\dagger \mathbf{s} \cdot (\mathbf{d}_{ij}^1 \times \mathbf{d}_{ij}^2) c_j. \quad (25)$$

Here a is the size of the cubic unit cell, t represents the hopping, and λ_{SO} represents the spin-orbit coupling. The first term represents the nearest neighbor hopping, and the second term is a spin-dependent hopping to the next nearest neighbor sites. \mathbf{d}_{ij}^1 and \mathbf{d}_{ij}^2 are the vectors for the two nearest neighbor bonds included in the next-nearest-neighbor hopping.

This four-band model is \mathcal{I} -reversal and time-reversal symmetric. It means that every eigenstate is doubly degenerate by the Kramers theorem. The doubly-degenerate conduction and the valence bands touch at the three X points, $X^r = (2\pi/a)\hat{r}$ ($r = x, y, z$), and therefore the bulk gap vanishes. To consider the phases with a bulk gap, suppose one changes the nearest-neighbor hopping to be different for the four directions of nearest neighbor bonds t_i ($i = 1, 2, 3, 4$)¹². The system then opens a gap between the two doubly-degenerate bands, while the \mathcal{I} -reversal and time-reversal symmetries are preserved. In Ref. 12, the phase boundary is studied when the hopping is changed slightly from the identical value: $t_i = t + \delta t_i$. When we set $\delta t_3 = 0 = \delta t_4$, the phase diagram is as shown in Fig. 5(a) as a function of δt_1 and δt_2 as obtained in Ref. 12. Four phases meet at $\delta t_1 = 0 = \delta t_2$, where the system becomes gapless.

The problem of our current interest is how the phase boundary between the WTI and the STI changes when the \mathcal{I} -symmetry is broken. In the present model, the simplest way to break \mathcal{I} -symmetry is to introduce an alternating on-site energy λ_v , like in the 2D Kane-Mele (KM) model on the honeycomb lattice⁴. In the present 3D case, the alternating on-site energy reduces the system to be similar to the zincblende structure as in GaAs.

By introducing λ_v , the symmetry of the system is lowered, and an analytic calculation of the phase transition becomes much harder. In the present case, however, with a procedure explained in Appendix B, we can calculate how the WTI-STI phase transition changes by breaking the \mathcal{I} -symmetry by the λ_v term. In the \mathcal{I} -symmetric ($\lambda_v = 0$) case, from the phase diagram (Fig. 5(a)) we consider $\delta t_+ = \delta t_1 + \delta t_2$ as a parameter m driving the phase transition, while $\delta t_1 - \delta t_2$ is fixed to be a nonzero value, for example, $\delta t_1 - \delta t_2 = 0.1t$. This corresponds to the red arrow in Fig. 5(a). The phase diagram in the δt_+ - λ_v plane is as given by Fig. 5(b). When the \mathcal{I} -symmetry is broken ($\lambda_v \neq 0$), the gapless region appears in the

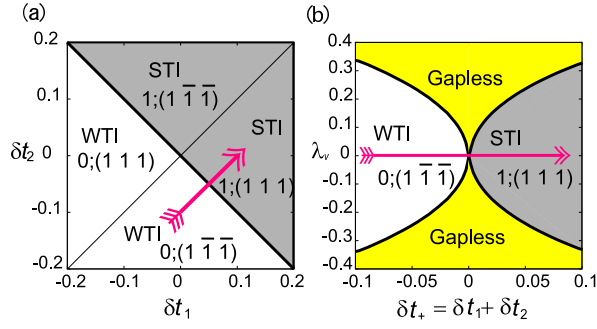


FIG. 5: (Color online) Phase diagrams for the Fu-Kane-Mele model with $\delta t_3 = 0$, $\delta t_4 = 0$. t_1 and t_2 are the bonds along the $[111]$ and $[\bar{1}\bar{1}\bar{1}]$ directions. We put $\lambda_{\text{SO}} = 0.1t$. The axes are in the unit of t . (a) The phase diagram in δt_1 - δt_2 plane obtained in Ref. 12. λ_v is set as zero. Each phase is indexed by cubic Miller indices, following Ref. 12. (b) The phase diagram in the δt_+ - λ_v plane. λ_v is newly introduced into the Fu-Kane-Mele model. Here $\delta t_+ = \delta t_1 + \delta t_2$, while we fix $\delta t_- = \delta t_1 - \delta t_2 = 0.1t$. The arrows (red) in (a) and (b) correspond to the identical change in parameters.

phase diagram. This confirms our theory in the previous section. As we explicitly show at the end of Appendix B, even when the model parameters are changed perturbatively, the gapless points move but never disappear. In this sense the gapless phase is stable.

To confirm our theory further, we calculate the trajectory (“string”) of the gapless points in \mathbf{k} space. As the parameter δt_+ is changed along the arrow in Fig. 6(b), the gapless points move in \mathbf{k} space, as shown in Fig. 6(a). As a whole, the trajectory is almost circular (but not exactly) in the \mathbf{k} space, around the X^x point. Note that when we gradually decrease λ_v , the trajectory is reduced to the X^x point.

The change in the Z_2 topological numbers can be seen by counting the intersection points between the trajectory and the planes $S_i^{(n_i)}$. We choose the reciprocal lattice vectors as $\mathbf{b}_1 = \frac{2\pi}{a}(-1, 1, 1)$, $\mathbf{b}_2 = \frac{2\pi}{a}(1, -1, 1)$, and $\mathbf{b}_3 = \frac{2\pi}{a}(1, 1, -1)$. The X^x point ($= (\mathbf{b}_2 + \mathbf{b}_3)/2 = \Gamma_{(011)}$) then lies on the planes $S_1^{(0)}$, $S_2^{(1)}$, and $S_3^{(1)}$, and the trajectory intersects these planes twice. The trajectory does not intersect the planes $S_1^{(1)}$, $S_2^{(0)}$, $S_3^{(0)}$. This means that among the Z_2 topological numbers, only ν_0 , ν_2 and ν_3 changes.

In the previous section we predicted that the dispersion at the pair creation and annihilation is anisotropic. To check this, we pick up a point of pair annihilation (Fig. 7), and calculate the dispersion around this point. Indeed, along the directions \mathbf{N}_1 and \mathbf{N}_2 the dispersion is linear; meanwhile, along the direction \mathbf{L} which is tangential to the trajectory of the monopole and the antimonopole, the dispersion is much softer and quadratic. This agrees with the theory in the previous section.

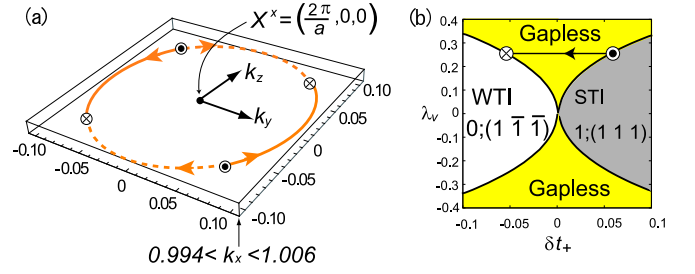


FIG. 6: (Color online) (a) Trajectory of the gapless points in \mathbf{k} space, as we change the parameter δt_+ with λ_v fixed. The wavenumber \mathbf{k} is shown in the unit of $(2\pi/a)$. The solid and broken curves are the trajectories for the monopoles and antimonopoles, respectively. This corresponds to the arrow in the phase diagram in (b).

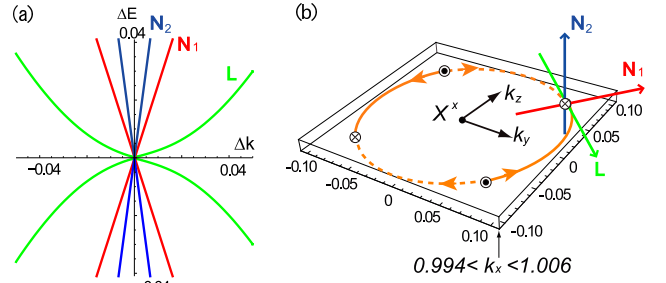


FIG. 7: (Color online) (a) Dispersion around the gapless points when the monopole-antimonopole pairs annihilate, for the Fu-Kane-Mele model. The direction \mathbf{L} is along the trajectory of the monopole and the antimonopole, while \mathbf{N}_1 and \mathbf{N}_2 are perpendicular to \mathbf{L} . These directions are shown in (b) in the trajectory for the gapless point in the \mathbf{k} space. Energy is shown in the unit t , and the wavenumber is in the unit $2\pi/a$.

IV. CONCLUSIONS AND DISCUSSIONS

In this paper, we described the generic phase diagrams involving the quantum spin Hall and insulator phases, by tuning an external parameter in 2D and 3D. In \mathcal{I} -asymmetric 3D systems, there lies a finite region of the gapless phase in the phase diagram. This was checked for the Fu-Kane-Mele model. We described the phase transition in terms of the motion of the gap-closing points (i.e. monopoles and antimonopoles) in \mathbf{k} space. The gapless phase in the \mathcal{I} -asymmetric 3D system originates from the conservation of “monopole charge”

We also studied the dispersion around the gapless points. In general the energy dispersion is linear around the gapless points. Meanwhile, around the gapless points at monopole-antimonopole pair creation/annihilation, the dispersion becomes quadratic in one direction of \mathbf{k} , which is tangential to the monopole trajectory.

It is interesting to compare the physics of gap-closing in the QSH phase and that in the quantum Hall (QH) phase. In the QH phase the bulk is gapped, and is characterized by the Chern number, by which this phase is distinct from

an ordinary insulator. For the QH phase, the behavior of monopoles and antimonopoles are quite similar to that presented so far in this paper. This point can be illustrated by using a 2D model of the quantum (anomalous) Hall effect proposed by Haldane²⁷. The phase diagram is shown in Ref. 27, where the transition between the QSH and the insulator phases occurs by changing the model parameter M . This phase transition occurs when the gap closes only at one wavenumber in the Brillouin zone, which is similar to the case of the 2D QSH phase¹⁶. In 3D, the gapless phase is expected to occur between the QH phase and the ordinary insulator phase (and also between two QH phases with different Chern numbers). It is because the symmetry class is unitary, and it is similar to the QSH phase without \mathcal{I} -symmetry. The 3D QH phase is characterized by three Chern numbers²⁸. Therefore, for the transition between phases with different sets of Chern numbers, a gapless phase is expected to appear in between. This gapless phase is described by a gapless loop C in the (m, \mathbf{k}) space, as in the 3D QSH case. The topology of the loop C relative to the crystallographic directions determines the change in the three Chern numbers at the transition. By comparing the cases of the QSH phase and the QH phase, they are different in the following aspects. First, the QH effect is without time-reversal symmetry. This makes the physics at \mathbf{k} and $-\mathbf{k}$ independent, in contrast with the QSH case. Therefore, the presence or absence of the \mathcal{I} -symmetry is inessential in the QH system. Second, because the QH system usually requires a strong magnetic field, and the motion parallel to the magnetic field is usually gapless, the QH phase in 3D is not easily realized in real systems. Meanwhile there is no such constraint for the QSH phase, and 3D QSH phase is easily realized. Thus the 3D gapless phase due to the topological nature of monopoles is more realistic in the QSH phase than in the quantum Hall phase.

When disorder is introduced in the system, the phase transition in three dimensions will have a gapless region as a function of the external parameter m . In 3D, only for \mathcal{I} -symmetric systems, the disorder effect on the phase transition between the QSH and I phases has been studied²⁹, while the \mathcal{I} -asymmetric systems are left to be analyzed. By regarding the whole system as one unit cell (“supercell”), the similar discussion holds. We impose the periodic boundary conditions, but with allowing additional phase twisting for the individual directions as θ_x , θ_y and θ_z . This phase twisting plays the role of the wavenumbers k_x , k_y and k_z . In this case, as the disorder generally breaks the \mathcal{I} -symmetry, the disorder brings about a gapless phase. This is an interesting question, and is beyond the scope of the present paper.

Acknowledgments

We are grateful to R. Shindou, L. Balents, and X.-L. Qi for fruitful discussions. This research is supported in

part by Grant-in-Aids from the Ministry of Education, Culture, Sports, Science and Technology of Japan.

APPENDIX A: GENERAL DESCRIPTION OF THE GAP-CLOSING POINTS IN m - \mathbf{k} SPACE

In this Appendix we assume that the bands are non-degenerate almost everywhere in \mathbf{k} space. It allows existence of isolated \mathbf{k} points with band degeneracy; meanwhile, the degeneracy in an extended region in \mathbf{k} space, such as Kramers degeneracy in systems with \mathcal{I} - and time-reversal symmetry is excluded. The vectors $\mathbf{A}_\alpha(\mathbf{k})$, $\mathbf{B}_\alpha(\mathbf{k})$ are defined in the three-dimensional \mathbf{k} space. To study behaviors of the gap-closing point by changing m , it is convenient to consider a four-dimensional (m, \mathbf{k}) space. Let us write

$$k_0 \equiv m, \quad (\text{A1})$$

and we define the following 4-vectors

$$A_{\alpha,i}(k) \equiv A_{\alpha,i}(m, \mathbf{k}) = -i \langle \psi_\alpha(m, \mathbf{k}) | \frac{\partial}{\partial k_i} | \psi_\alpha(m, \mathbf{k}) \rangle, \quad (\text{A2})$$

$$B_{\alpha,ij}(k) \equiv B_{\alpha,ij}(m, \mathbf{k}) = \frac{\partial}{\partial k_i} A_{\alpha,j}(m, \mathbf{k}) - \frac{\partial}{\partial k_j} A_{\alpha,i}(m, \mathbf{k}), \quad (\text{A3})$$

where $k = (k_0, k_1, k_2, k_3) = (m, \mathbf{k})$ and $i = 0, 1, 2, 3$. This corresponds to the vectors in Eqs. (3)(4) as $\mathbf{A}_\alpha(\mathbf{k}) = (A_1, A_2, A_3)$, $\mathbf{B}_\alpha(\mathbf{k}) = (B_{23}, B_{31}, B_{12})$. We omit the band index α henceforth, unless necessary. The monopole density $\rho(\mathbf{k})$ becomes a 4-vector $\rho = (\rho_0, \rho_1, \rho_2, \rho_3)$, where

$$\rho_l = \frac{1}{2\pi} \epsilon_{lijk} \frac{\partial}{\partial k_i} \frac{\partial}{\partial k_j} A_k. \quad (\text{A4})$$

and ϵ_{lijk} is the totally antisymmetric tensor with $\epsilon_{0123} = 1$. We note that $\rho(\mathbf{k}) = \rho_0$. From Eq. (A4), if the band α is not degenerate with other bands at (m, \mathbf{k}) , $A_i(k)$ is analytic, and $\rho_l(m, \mathbf{k})$ identically vanishes. This does not apply when the band is degenerate with other bands at some \mathbf{k} points; at such degenerate points, ρ_l has a δ -function singularity, as we see below. Such points form a curve in (m, \mathbf{k}) space because the gapless condition consists of three equations, i.e. the codimension is three^{18,19} in this case. We call this gapless curve as a “string”. We will see that the 4-vector ρ describes a current inside the string, and the total “current” inside the string is an integer. In general this “current” is unity.

To see how the singularity appears, we show the following; (a) a surface integral of ρ_l over a closed three-dimensional hypersurface V in (m, \mathbf{k}) space is zero (i.e. ρ is divergence-free), and (b) a surface integral of ρ_l over an open 3-dimensional hypersurface \tilde{V} in (m, \mathbf{k}) space is quantized. To see (a) we use the Gauss theorem.

$$\int_V d\sigma^{ijk} \epsilon_{lijk} \rho_l = \frac{1}{2\pi} \int_{\partial V} d\sigma^{jk} \frac{\partial}{\partial k_j} A_k = 0, \quad (\text{A5})$$

because ∂V is null. This proof relies on the fact that $B_{jk} = \frac{\partial}{\partial k_j} A_k - \frac{\partial}{\partial k_k} A_j$ is gauge invariant. Next we show (b).

$$\frac{1}{3!} \int_{\partial \tilde{V}} d\sigma^{ijk} \epsilon_{lijk} \rho_l = \frac{1}{2\pi} \int_{\partial \tilde{V}} d\sigma^{jk} \frac{\partial}{\partial k_j} A_k \quad (\text{A6})$$

This quantity is an integer, representing a monopole charge inside $\partial \tilde{V}$. To show this we use the Stokes theorem to this expression. In general, when the closed two-dimensional surface $\partial \tilde{V}$ encloses a degeneracy point, the field A_k cannot be expressed as a single function on the surface $\partial \tilde{V}$. Thus the Stokes theorem can only be applied after dividing the surface $\partial \tilde{V}$ into pieces, on each of which the wavefunction (and the field A_i) is continuous²⁴. The resulting formula is expressed in terms of a phase difference between the neighboring pieces. Because the phase of the wavefunctions allows a difference of a multiple of 2π , this quantity becomes an integer. Thus from (a)(b), we have shown that ρ_l describes a (divergence-free) “current” in the string, with its current being quantized inside the string. This kind of discussion with patching of the wavefunction is discussed in the context of the Berry phase^{22,23}, and also in the context of the quantum Hall effect²⁴, and magnetic superconductor³⁰.

The expression of ρ_l is therefore given by

$$\rho_l = \int ds \frac{dK_l(s)}{ds} \delta^{(4)}(k - K(s)) \quad (\text{A7})$$

where $K(s) = (K_0(s), K_1(s), K_2(s), K_3(s)) = (M(s), \mathbf{K}(s))$ describes a trajectory (i.e. string) of the gap-closing point in the 4-dimensional space, s is a parameter along the string, and $\delta^{(4)}(k - K(s)) = \prod_{i=0}^3 \delta(k_i - K_i(s))$. The divergence becomes zero because

$$\begin{aligned} \frac{\partial \rho_l}{\partial k_l} &= \int ds \frac{dK_l(s)}{ds} \frac{\partial}{\partial k_l} \delta^{(4)}(k - K(s)) \\ &= - \int ds \frac{dK_l(s)}{ds} \frac{\partial}{\partial K_l} \delta^{(4)}(k - K(s)) \\ &= - \int ds \frac{d}{ds} \delta^{(4)}(k - K(s)) = 0. \end{aligned} \quad (\text{A8})$$

The 0-th component of (A7) gives

$$\begin{aligned} \rho(m, \mathbf{k}) &= \int ds \frac{dM(s)}{ds} \delta(m - M(s)) \delta^{(3)}(\mathbf{k} - \mathbf{K}(s)) \\ &= \sum_{s_i: m=M(s_i)} \text{sgn} \left(\frac{dM(s)}{ds} \right)_{s=s_i} \delta^{(3)}(\mathbf{k} - \mathbf{K}(s_i)), \end{aligned} \quad (\text{A9})$$

where the summation is taken over $s = s_i$ which satisfies $m = M(s_i)$ for given m . By equating this with

$$\rho(m, \mathbf{k}) = \sum_{s_i: m=M(s_i)} q_i \delta^{(3)}(\mathbf{k} - \mathbf{K}(s_i)), \quad (\text{A10})$$

we get the monopole charge to be $q_i = \text{sgn} \left(\frac{dM(s)}{ds} \right)_{s=s_i}$. This means that when the “current” in the string is going

in the increasing direction of m , it appears as a monopole ($q = 1$), whereas the decreasing direction of m corresponds to an antimonopole ($q = -1$), as shown in Fig. 8

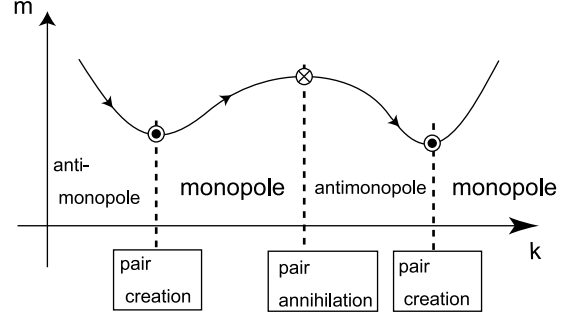


FIG. 8: The string which is a set of gapless points in the (m, \mathbf{k}) space. The arrow describes the direction of the flow vector ρ .

We now return to the present case of the transition between the QSH and the insulator phases. Recall that the string is confined in a restricted region $m_1 \leq m \leq m_2$ in the m direction. Therefore the “string” becomes a “loop”. Then it follows that at $m = m_1$ the “string” changes its direction in the m space, which appears as a pair creation of monopole and antimonopole. Similarly at $m = m_2$ a pair annihilation of monopole and antimonopole results.

In the particular cases with time-reversal invariance, as we are interested in, the pair creation and pair annihilation appears symmetrically with respect to $\mathbf{k} = \mathbf{\Gamma}_i$. Therefore, we expect that the number of loops should be one in the simplest case will be as shown in Fig. 3, and it is indeed realized in the Fu-Kane-Mele model with the λ_v term.

APPENDIX B: CALCULATION OF THE GAPLESS PHASE IN THE FU-KANE-MELE MODEL WITH STAGGERED ON-SITE POTENTIAL

The Hamiltonian matrix for the the Fu-Kane-Mele model with staggered on-site potential λ_v is written as

$$H(\mathbf{k}) = \begin{pmatrix} \lambda_v \mathbf{1} + \sum_{i=1}^3 F_i \sigma_i & F_0 \mathbf{1} \\ F_0^* \mathbf{1} & -\lambda_v \mathbf{1} - \sum_{i=1}^3 F_i \sigma_i \end{pmatrix} \quad (\text{B1})$$

where σ_i are the Pauli matrices, and $\mathbf{1}$ is the 2×2 identity matrix. The coefficients are given by

$$F_0 = t_1 e^{ia(k_y + k_z)/2} + t_2 e^{ia(k_z + k_x)/2} + t_3 e^{ia(k_x + k_y)/2} + t_4, \quad (\text{B2})$$

$$F_x = -4\lambda_{\text{SO}} \sin \frac{k_x a}{2} \left(\cos \frac{k_z a}{2} - \cos \frac{k_y a}{2} \right), \quad (\text{B3})$$

and F_y, F_z are given similarly to F_x after cyclic permutation of the subscripts x, y and z . We write $\mathbf{F} =$

(F_x, F_y, F_z) for brevity. We study when and how the gap closes as the parameters change. Because the gap is between the second and the third bands, we need a condition when the second and third bands have identical eigenenergies. As the codimension is three in this case, the condition should be expressed as three equations, determining a string in (m, \mathbf{k}) space. First we note that the spectrum of H is symmetric with respect to $E = 0$, as follows from

$$UH(\mathbf{k})U^{-1} = -^t H(\mathbf{k}), \quad (\text{B4})$$

where the superscript t denotes matrix transposition, and the unitary matrix U is given by

$$U = \sigma_y \otimes \mathbf{1} = \begin{pmatrix} & -i & \\ i & & \\ & i & \end{pmatrix}. \quad (\text{B5})$$

Thus the gap closes if and only if one of the eigenvalues of H vanishes, namely, $\text{Det}H(\mathbf{k}) = 0$. This renders to

$$|F_0|^4 + 2|F_0|^2(\lambda_v^2 + |\mathbf{F}|^2) + (\lambda_v^2 - |\mathbf{F}|^2)^2 = 0, \quad (\text{B6})$$

namely,

$$\text{Re}F_0 = 0, \text{Im}F_0 = 0, \lambda_v^2 = |\mathbf{F}|^2. \quad (\text{B7})$$

For given model parameters t_i, λ_v , the coupled equations (B7) gives gapless points in \mathbf{k} -space, if any. Such gapless points are stable against small changes of parameters, as we can see as follows. For brevity, let us write the three conditions in Eq. (B7) as $g_i(\mathbf{k}, \mathbf{t}) = 0$ ($i = 1, 2, 3$), where \mathbf{t} denotes the set of model parameters. Let \mathbf{k}_0 be the wavenumber of one of the gapless points. When the model parameters are changed, the values of g_i change accordingly: $g_i \rightarrow g_i + \delta g_i$. The gapless points are then expected to move ($\mathbf{k} = \mathbf{k}_0 \rightarrow \mathbf{k} = \mathbf{k}_0 + \delta \mathbf{k}_0$). Because the gapless conditions are expanded as

$$\nabla_{\mathbf{k}} g_i(\mathbf{k}_0) \cdot \delta \mathbf{k}_0 + \delta g_i(\mathbf{k}_0) = 0, \quad (\text{B8})$$

there always exists $\delta \mathbf{k}_0$ satisfying these three coupled linear equations. Thus a perturbative change in system parameters moves the gapless points in \mathbf{k} -space, without removing them.

In particular, when $\lambda_v = 0$, the system is \mathcal{I} -symmetric. The third condition in Eqs. (B7) then gives the wavenumber \mathbf{k} to be one of the X' points; the other conditions lead us to the phase diagram in Ref. 12 (also in Fig. 5(a)) easily.

* Electronic address: murakami@stat.phys.titech.ac.jp

¹ S. Murakami, N. Nagaosa, and S.-C. Zhang, *Science* **301**, 1348 (2003).

² J. Sinova, D. Culcer, Q. Niu, N. A. Sinitsyn, T. Jungwirth, and A. H. MacDonald, *Phys. Rev. Lett.* **92**, 126603 (2004).

³ S. Murakami, N. Nagaosa, and S.-C. Zhang, *Phys. Rev. Lett.* **93**, 156804 (2004).

⁴ C. L. Kane and E. J. Mele, *Phys. Rev. Lett.* **95**, 146802 (2005).

⁵ C. L. Kane and E. J. Mele, *Phys. Rev. Lett.* **95**, 226801 (2005).

⁶ B. A. Bernevig and S.-C. Zhang, *Phys. Rev. Lett.* **96**, 106802 (2006).

⁷ C. Wu, B. A. Bernevig, and S.-C. Zhang, *Phys. Rev. Lett.* **96**, 106401 (2006).

⁸ C. Xu and J. E. Moore, *Phys. Rev. B* **73**, 045322 (2006).

⁹ S. Murakami, *Phys. Rev. Lett.* **97**, 236805 (2006).

¹⁰ B. A. Bernevig, T. L. Hughes, S.-C. Zhang, *Science* **314**, 1757 (2006).

¹¹ M. König, S. Wiedmann, C. Brüne, A. Roth, H. Buhmann, L. W. Molenkamp, X.-L. Qi, and S.-C. Zhang *Science* **318**, 766-770 (2007).

¹² L. Fu, C. L. Kane, and E. J. Mele, *Phys. Rev. Lett.* **98**, 106803 (2007).

¹³ J. E. Moore and L. Balents, *Phys. Rev. B* **75**, 121306(R) (2007).

¹⁴ D. Hsieh, D. Qian, L. Wray, Y. Xia, Y. S. Hor, R. J. Cava and M. Z. Hasan, *Nature* **452**, 970 (2008).

¹⁵ L. Fu and C. L. Kane, *Phys. Rev. B* **74**, 195312 (2006).

¹⁶ S. Murakami, S. Iso, Y. Avishai, M. Onoda, and N. Nagaosa, *Phys. Rev. B* **76**, 205304 (2007).

¹⁷ S. Murakami, *New J. Phys.* **9**, 356 (2007); (Corrigendum) *ibid.* **10**, 029802 (2008).

¹⁸ V. J. von Neumann and E. Wigner, *Physik. Zeitschr.* **30**, 467 (1929).

¹⁹ C. Herring, *Phys. Rev.* **52**, 361; *ibid.* **52**, 365 (1937).

²⁰ E. P. Wigner, *Ann. Math.* **67**, 325 (1958).

²¹ F. J. Dyson, *J. Math. Phys.* **3**, 140 (1962).

²² M. V. Berry, *Proc. Roy. Soc. London Ser. A* **392**, 45 (1984).

²³ G. E. Volovik, *The Universe in a Helium Droplet*, (Oxford University Press, Oxford, 2003).

²⁴ M. Kohmoto, *Ann. Phys.* **160**, 343 (1985).

²⁵ T. T. Wu and C. N. Yang, *Phys. Rev. D* **12**, 3845 (1975).

²⁶ S. Raghu, X.-L. Qi, C. Honerkamp and S.-C. Zhang, *Phys. Rev. Lett.* **100**, 156401 (2008).

²⁷ F. D. M. Haldane, *Phys. Rev. Lett.* **61**, 2015 (1988).

²⁸ G. Montambaux and M. Kohmoto, *Phys. Rev. B* **41**, 11417 (1990).

²⁹ R. Shindou and S. Murakami, arXiv:0808.1328.

³⁰ S. Murakami and N. Nagaosa, *Phys. Rev. Lett.* **90**, 057002 (2003).